

# Large Eddy Simulation in a Channel with Exit Boundary Conditions

*T. Cziesla, H. Braun, G. Biswas\*, N. K. Mitra†*  
*Institut für Thermo- und Fluidodynamik*  
*Ruhr-Universität Bochum*  
*44780 Bochum, Germany*

## Abstract

The influence of the exit boundary conditions (vanishing first derivative of the velocity components and constant pressure) on the large eddy simulation of the fully developed turbulent channel flow has been investigated for equidistant and stretched grids at the channel exit.

Results show that the chosen exit boundary conditions introduce some small disturbance which is mostly damped by the grid stretching. The difference between the fully developed turbulent channel flow obtained with LES with periodicity condition and the inlet and exit and the LES with fully developed flow at the inlet and the exit boundary condition is less than 10% for equidistant grids and less than 5% for the case grid stretching. The chosen boundary condition is of interest because it may be used in complex flows with backflow at exit.

---

\*Department of Mechanical Engineering, IIT, Kanpur, India.

†This research was supported by the National Aeronautics and Space Administration under NASA Contract No. NAS1-19480 while the fourth author was in residence at the Institute for Computer Applications in Science and Engineering (ICASE), NASA Langley Research Center, Hampton, VA 23681-0001.

## Introduction

Large eddy simulation of turbulent channel flows has been reported first by Kim and Moin [8] who considered a fully developed turbulent flow, for which periodicity conditions at the inlet and the exit of the computational domain can be assumed. The great advantages are that the problem of specification of the exit boundary condition can be avoided. The exit boundary condition for direct and large eddy simulation of turbulent flows plays a more important role with respect to damping than for laminar flows. However, in real flows the periodicity condition is more the exception than the rule. For example, for jet or impinging jet flows no periodicity condition can be used at the exit. Some research has been reported on the use of non-periodic exit conditions.

Werner [18] used vanishing first or second derivative conditions for the velocity-components:

$$\frac{\partial^l U_i}{\partial x_i^l} = 0; \quad l = 1 \quad \text{or} \quad 2 \quad (1)$$

With this von-Neumann-type-boundary-condition he calculated turbulent channel flows by using the Smagorinsky-Lilly [16] model. This kind of boundary condition is often used for laminar flows, where only spatially smooth fields of flow values like velocity, pressure with very small gradients exist. This means that further spatial development of flow is negligibly small.

Werner [18] pointed out that a very smooth field can be represented in Fourier space as one wave with large wavelength and some waves with negligibly small wavelength. The difference form of vanishing first derivative corresponds exactly to waves with infinite wavelengths. The difference form of the vanishing second derivative with equidistant grids corresponds to a wave of infinite length and a wave with finite length, which is large in comparison to the grid distances. In contrast to laminar flows one can find very large gradients in turbulent flows, i.e., very rough fields. So there are also waves with short wavelengths, which are

reflected at the exit boundary. These reflections mean a disturbance of the results of the computational domain. Finally it should be mentioned, that vanishing higher derivatives as exit condition can lead to numerical instabilities [18]. An alternative class of boundary conditions are the so-called “Non-Reflecting-Boundary-Conditions” which were originally developed for hyperbolic equations [3-6]. Jin and Braza [7] used such a condition for an elliptic problem. They calculated the transition of free shear layers using the two dimensional incompressible unsteady Navier-Stokes equations.

The basic idea of their boundary condition formulation is the requirement that the waves of short length could pass through the boundary without being reflected. Basing on the 2D wave equation

$$\frac{\partial^2 u_i}{\partial t^2} - c_x^2 \frac{\partial^2 u_i}{\partial x^2} - c_y^2 \frac{\partial^2 u_i}{\partial y^2} = 0 \quad (2)$$

they developed the following equation:

$$\frac{\partial u_i}{\partial t} - u_1 \frac{\partial u_i}{\partial x} - v \frac{\partial^2 u_i}{\partial y^2} = 0 \quad (3)$$

where  $u_1$  is the velocity in the main flow direction.

Comparison of the coefficients of this equation with the Navier-Stokes equation provides the matched form of equation [3].

Another formulation of non-reflecting boundary condition is presented by Bestek [2] for the investigation of transition of boundary layers, from the solution of the velocity-vorticity formulation of Navier-Stokes equations. The second derivatives in the main flow direction (normal to the exit plane) are set to zero. So there is a damping which leads to relaminarization of the flow near the exit plane and reflection of disturbances is decreased.

Richter et al. [13, 14] have used “frozen turbulence” as the boundary condition in flows with pressure gradient. This technique is based on the assumption that the time variation of the turbulent fluctuations (the difference of instantaneous values of the flow variables from their average values) depend on the convective transport, i.e., the instantaneous values at the exit plane depend on the ones directly at the upstream. Richter et al. [13, 14] developed a relationship between the fluctuations at the exit plane and the plane directly upstream of the exit:

$$\Phi''(n_x, j, k) |_{n} = \Phi''(il, j, k) |_{n-\Delta n} \quad (4)$$

$$\Delta n(j, k) = \frac{\Delta x}{[\Delta t \cdot u_c(j, k)]} \quad (5)$$

where  $u_c$  is the characteristic convective velocity at the exit in  $x$ -direction and is set equal to  $\langle u(il, j, k) \rangle$ , where  $\langle \rangle$  symbolizes the time averaged value. It is necessary to save enough time levels ( $\Delta n$  levels for getting  $\Phi'' |_{n-\Delta n}$ ) for implementation of this boundary condition. With the following equation

$$\Phi(i, j, k) = \tilde{\Phi}[i, j, k] + \Phi''(i, j, k) \quad (6)$$

the values at the exit plane can be defined. The average value  $\Phi$  is calculated by using a linear extrapolation of the variables from the interior points.

The purpose of the present work is to perform LES for fully developed turbulent flows in a rectangular channel with an exit boundary condition and compare the results with computations with periodicity conditions in order to determine the influence of the boundary condition (see Fig. 1). The underlying idea is that for the channel with exit boundary condition the flow at the entrance is fully-developed turbulence. We would expect the

turbulence to remain fully developed and our chosen exit boundary condition should have negligible effect on the flow.

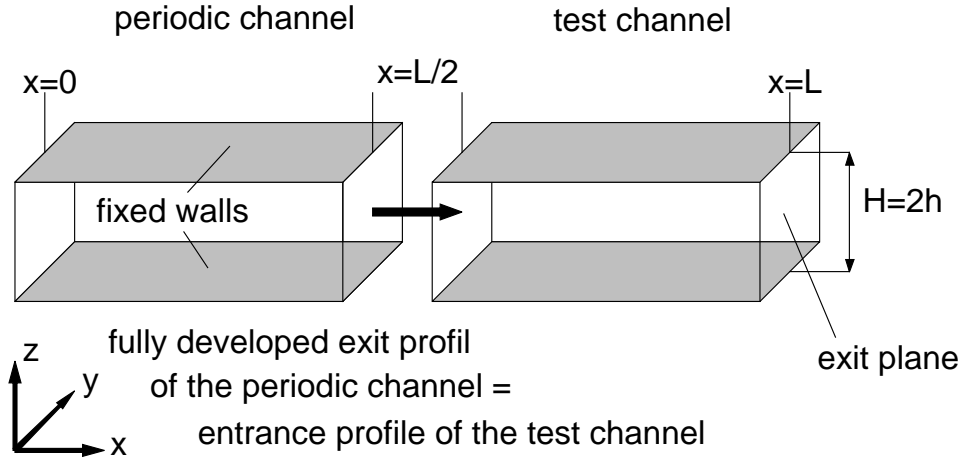


**Fig. 1:** Schematic of the geometry

As boundary condition we decided to use the vanishing first derivative condition like Werner [18] described above. One important aspect for this choice was the experience [9], that this condition in principle allows the calculation of complex flow structures like backflow at the exit plane caused by the entrainment. So it is interesting to investigate such a condition because there are no exact formulations for the LES of such kind of flows (like jets, impinging jets etc.) so far, where the flow is nonperiodic and a back flow appears at the nominal exit. Jin and Braza [7] showed indeed good results for the simulation of the 2D Navier-Stokes equations for transitional free shear flow. But it is not known if their non-reflecting condition is suitable for calculating 3D turbulent flows by LES as well. Beside their boundary condition will not allow backflow at the exit plane. The same is true for the condition used by Bestek [2]. The “frozen turbulence” condition from Richter et al. [13, 14] is expensive because of the necessity of large computer time for sampling the variables at different time levels.

## Numerical Method

We consider a rectangular channel of length  $L$ , see Fig. 1. We use periodicity boundary conditions at  $x = 0$  and  $x = L/2$  so that fully developed turbulent flow is simulated. Then the computation is further continued to  $x = L$  where the exit boundary condition is used. A comparison of the flow field at the first half and at second half of the channel would show the influence of the exit boundary condition (see Fig. 1).

The basic equations are

$$\frac{\partial \bar{u}_i}{\partial x_i} = 0 \quad (7)$$

$$\frac{\partial \bar{u}_i}{\partial t} = -\frac{\partial \bar{p}}{\partial x_i} - \frac{\partial \bar{u}_i \bar{u}_j}{\partial x_j} - \frac{\partial \overline{u_i u_j}}{\partial x_j} + \frac{1}{Re} \frac{\partial^2 \bar{u}_i}{\partial x_j^2}$$

For the subgrid scales the Smagorinsky-Lilly model is used (with  $C_s = 0.1$ ).

$$-\overline{u_i u_j} = 2\bar{\nu}_{ij} \bar{S}_{ij} - \frac{1}{3} \overline{u_k u_k} \delta_{ij} \quad (8)$$

$$\bar{\nu}_t = (c_s \cdot \Delta)^2 \sqrt{2S_{ij} S_{ij}} \quad (9)$$

$$\bar{S}_{ij} = \frac{1}{2} \left[ \frac{\partial \bar{u}_i}{\partial x_j} + \frac{\partial \bar{u}_j}{\partial x_i} \right] \quad (10)$$

## Boundary Conditions

No-slip conditions have been used on the walls for the convective terms. The no-slip condition for the diffusive terms were implemented by using the Schumann-assumption [15] in coupling

with the logarithmic law of the wall. Periodicity conditions have been used at  $x = 0$  and  $x = L/2$ . At  $x = L$  we use

$$\frac{\partial u_i}{\partial x_i} = 0 \tag{11}$$

and

$$p = \text{constant} \tag{12}$$

Use of the coupled vanishing first derivative boundary condition with  $p = \text{const.}$  is based on an outflow boundary condition from Rannacher [12]. Our investigations showed that these conditions are suitable for the calculation of backflow caused by entrainment. The assumption of constant pressure is acceptable because at the exit plane the fluid leaves the computational domain towards the ambient flow where a constant pressure, namely the ambient pressure, exists. The handling of backflow is obviously one of the great problems for simulation of impinging jet flow etc., see Benocci [1]. Some authors presented conditions where a so-called buffer layer near to the exit plane (Benocci, [1]) or the assumption of vanishing first derivatives in main flow direction for the base flow [10] is necessary. But this enlarges the computational domain and thereby the computational time. Because we want to investigate impinging jet flows by LES in future we decided to use Eqs. (11) and (12).

## Method of Solution

The basic equations have been solved by a fractional step method following Kim and Moin [8] using Adams-Bashforth and Crank-Nicholson difference schemes and a SIP solver of Stone [17] for the numerical solution of the pressure Poisson equation.

## Results and Discussion

The Reynolds number based on the half of the channel height is

$$Re = \frac{u_m^* h^*/2}{\nu^*} = 2800, \quad (Re_\tau = 180) \quad (13)$$

$u_m$  is the average velocity in main flow ( $x$ -) direction. Each half of the channel was discretized with  $34 \times 34 \times 18 = 20808$  grids. The nondimensional length in the  $x$ -direction was 8.5 for each half, in the  $y$ -direction 4 and in the  $z$ -direction 2 ( $\Delta x = 0.25$ ,  $\Delta y = \Delta z = 0.125$ ).

In addition a modification of the boundary condition was done.

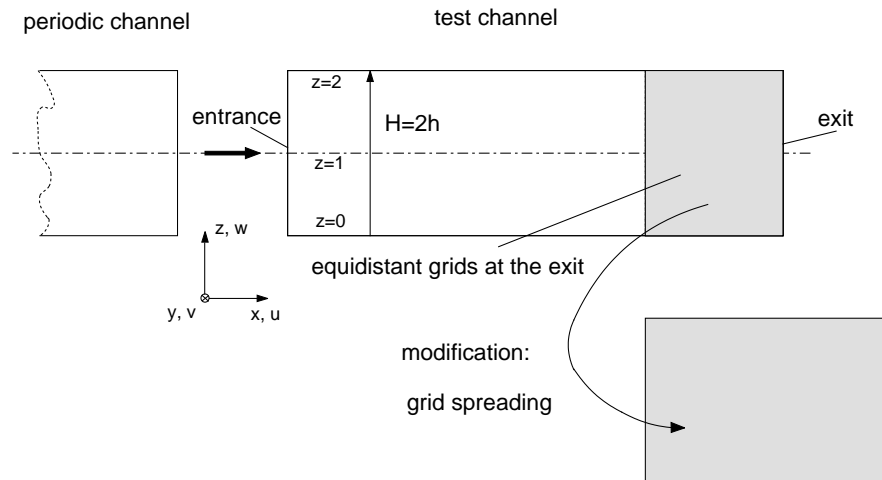


**Fig. 2:** Schematic of the computational scheme

The length of the second half of the channel, i.e., the part where we wanted to investigate the influence of the boundary condition, was increased to  $L = 9.145$  by stretching the last 8 grid cells in  $x$ -direction steadily by 10% of the grid distance of the upstream neighbouring cell (see Fig. 2). With this stretching, the numerical viscosity is increased. This stretching is probably equivalent to a buffer layer. The computations will also show if and how the nonequidistant grids would influence the results in comparison to the case of equidistant grids.

As results we show first the distributions of different root-mean-square(rms)-values. For the investigation of the influence of our boundary condition we divided the second half of the channel into two parts (each part with 17 grid cells), see Fig. 2, so that one can observe if and how the influence of the exit plane is transmitted in the upstream direction. Figures 3, 4 and 5 compare the distribution of the different rms values in the three directions. Obviously the rms values for the channel with our boundary conditions are higher than that of the periodic channel. The graphs of the channel half with our boundary conditions are nearly identical. This indicates an influence of the exit boundary condition through the whole channel. The graphs of the test cases show (in the periodic case) nearly constant deviation in the channel core and are identical in the wall region. In Table 1, the local maxima (max) and minima (min) of each rms-component of the periodic and the two parts of the test channel are compared. The differences of the each part of the second channel expressed in percent are related to the periodic channel. The values of the two parts of the test channel differ at both maxima and minima. But the largest difference, the rms-value in  $y$ -direction, is only 10.27%. All the other differences are lower. Our boundary condition introduces a disturbance in the whole test channel, which is expressed by higher rms values. But the effect of this disturbance is relatively low. Both parts of the test channel are influenced equally.

It should be mentioned, that the differences of the maximum rms values are smaller than the differences of the minimum values, see Table 1. This means that the locations of the flow where the fluctuation level is high are less influenced than locations where the level is low.

Figures 6-8 show the distribution of rms values for the case of grid spreading. The graphs of the first part of the test channel are above the ones of the periodic channel. The values of the second part are equal or, even lower at the maximum value than the ones of the periodic channel. This indicates a decrease of the fluctuations because of the damping effect of the grid spreading. Table 2 shows the maximum and minimum rms values and the differences of the two parts of the test channel from the periodic solutions. The mentioned tendencies can be confirmed again. The rms values of the first part are higher than that of the periodic channel, but lower than the ones for the case of equidistant grids, (see in Table 1). All the values of the second part are even lower than the values of the periodic channel. This means, that in case of grid spreading there is also an influence of the boundary condition. But compared to the case of equidistant grid a decrease of the differences with respect to the periodic calculation could be achieved. The reason is the increase of the damping effect by numerical viscosity because of the grid spreading. This spreading influences very strongly the calculation of the rms values of the second test channel half. In this part, the damping effect is larger. This explains the low rms values here. Besides, because of this damping the disturbance caused by the boundary condition cannot be reproduced as in case of equidistant grids. There is a decrease of the values in the first test channel part.

In Figs. 7 and 8 the Reynolds shear stresses at  $x - z$  plane (see Figures 1 and 2) are shown. Table 1 compares the maximum and minimum values of the Reynolds stresses. One can point out that the simulation using the present boundary condition give acceptable results. In case of equidistant grids the maximum difference from the periodic case for the local

maxima and minima is -6.17% (see Table 1, the negative sign results from the definition of the direction of the axis-system). The comparison of the averaged centerline velocity confirm this conclusion, see Table 4.

In case of grid spreading the results are even better, see Fig. 8 and Table 4. Here the maximum difference for the comparison of the local maxima and minima is only 2.40%. The comparison of the centerline velocities also show very good results, see Table 4.

## **Conclusion**

The influence of coupled exit boundary condition of a vanishing first derivative on LES of turbulent channel flows for the velocities and constant pressure was investigated. A comparison of the results with the case of using periodic boundary condition was done. Besides, a modification - continuously stretching of 8 grid cells near the exit plane - of the selected boundary condition was presented.

The results confirm the suspicion, that the disturbance caused by the boundary condition at the exit plane is transported in the upstream direction. The influence of the chosen boundary condition leads to slightly increased turbulent fluctuations. This behavior is expressed by higher rms values.

The results with grid spreading, because of the increased damping of non-equidistant grids, show better agreement with fully developed results.

It was also found that the disturbance caused by these boundary conditions are small where the flow fluctuates strongly. So one can expect that this boundary condition should give good results for other kinds of flow especially with high levels of turbulent fluctuations like impinging jets.

## Acknowledgement

We thank the Deutsche Forschungsgemeinschaft for financial support of this project.

## References

- [1 ] Benocci, G., Hoffmann, C.: Numerical Simulation of Spatially-Developing Planar Jets, Proceedings of the AGARD Fluid Dynamic Panel Symposium, Chania, Greece, April 18-21, 1994
- [2 ] Bestek, H., Kloker, M., Müller, W.: Spatial Direct Numerical Simulation of Boundary Layer Transition Under Strong Adverse Pressure Gradient, Proceedings of the 74th AGARD Fluid Dynamics Panel Symposium “Application of Direct and Large-Eddy Simulation to Transition and Turbulence”, Chania, Greece, April 18-21, 1994
- [3 ] Enquist, B., Majda, A.: Numerical Radiation Boundary Conditions for Unsteady Transonic Flow, Journal of Computational Physics, 40, 1981
- [4 ] Gustaffson, B., Kreiss, H.O.: Boundary Conditions for Time Dependent Problems with an Artificial Boundary, Journal of Computational Physics, 30, 1979
- [5 ] Han, T.Y., Meng, J.C.S., Innis, G.E.: An Open Boundary Condition for Incompressible Stratified Flows, Journal of Computational Physics, 49, 1983
- [6 ] Hedstrom, G.W.: Nonreflecting Boundary Conditions for Nonlinear Hyperbolic Systems, Journal of Computational Physics, 30, 1979
- [7 ] Jin, G., Braza, M.: A Nonreflecting Outlet Boundary Condition for Incompressible Unsteady Navier-Stokes Calculations, Journal of Computational Physics, 107, 1993
- [8 ] Kim, J., Moin, P.: Application of a Fractional-Step Method to Incompressible Navier-Stokes Equations, Journal of Computational Physics, 59, 1985

- [9 ] Laschefski, H.: Numerische Untersuchung der dreidimensionalen Strömungsstruktur und des Wärmeübergangs bei ungeführten und geführten Freistrahlen mit Prallplatte, Dissertation Ruhr-Universität Bochum, 1993
- [10 ] Nordström, J.: Accurate Solutions of the Navier-Stokes Equations Despite Unknown Boundary Data, *Journal of Computational Physics*, 120, Sept. 1995
- [11 ] Orlanski, I.: A Simple Boundary Condition for Unbounded Hyperbolic Flows, *Journal of Computational Physics*, 21, 1976
- [12 ] Rannacher, R.: On the Numerical Solution of the Incompressible Navier-Stokes Equations, Preprint 92 - 12 Universität Heidelberg, Vortrag auf der GAMM-Jahrestagung in Leipzig, 24.-27.3.1992
- [13 ] Richter, K.: Grobstruktursimulation Turbulenter Wandschichten mit Wärmetransport, Dissertation, Fakultät Maschinenwesen, Technische Universität München, 1988
- [14 ] Richter, K., Friedrich, R., Schmitt, L.: Large-Eddy Simulation of Turbulent Wall Boundary Layers with Pressure Gradient, Sixth Symposium on "Turbulent Shear Flows", September 7-9, 1987, Toulouse, France
- [15 ] Schumann, U.: Subgrid-Scale Model for Finite Difference Simulations of Turbulent Flows in Plane Channels and Annuli, *Journal of Computational Physics*, 18, 1975
- [16 ] Smagorinsky, J.S.: General Circulation Experiments with Primitive Equations. I. The Basic Experiment, *Monthly Weather Review* 91, 1963
- [17 ] Stone, H.L.: Iterative Solution of Implicit Approximations of Multidimensional Partial Differential Equations, *SIAM J. Numerical Analysis*, 5, 1968

- [18 ] Werner, H.: Grobstruktursimulation der turbulenten Strömung über eine querliegende Rippe in einem Plattenkanal bei hoher Reynoldszahl, Dissertation, Fakultät Maschinenwesen, Technische Universität München, 1991

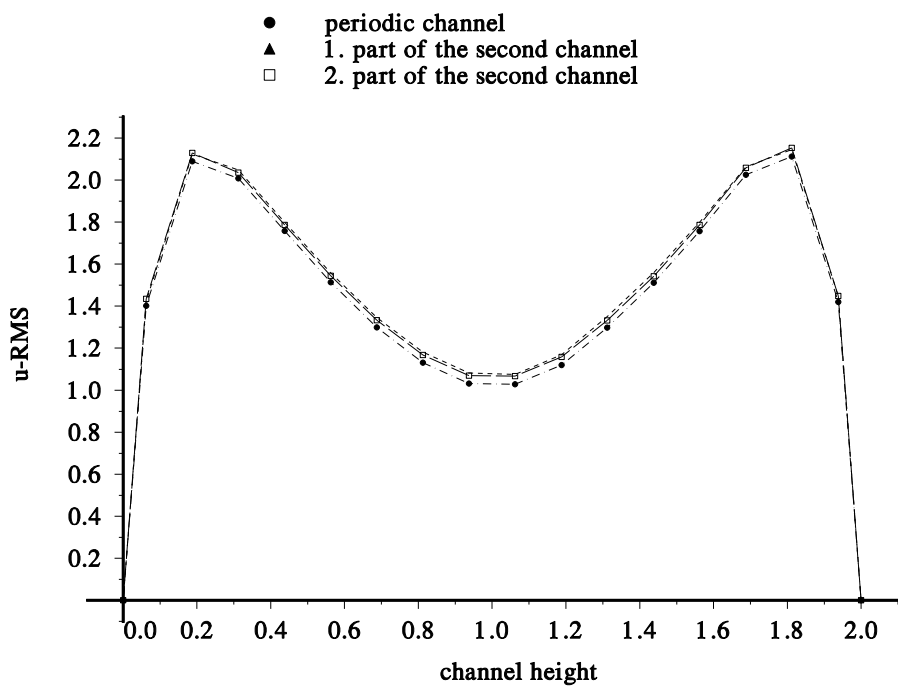


Fig. 3: u-rms, equidistant grid

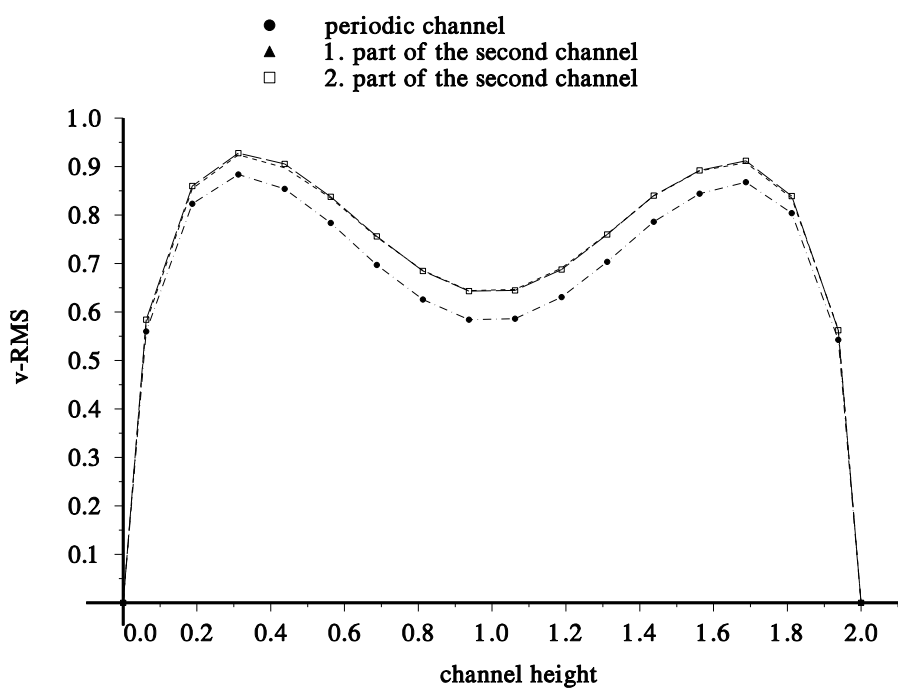


Fig. 4: v-rms, equidistant grid

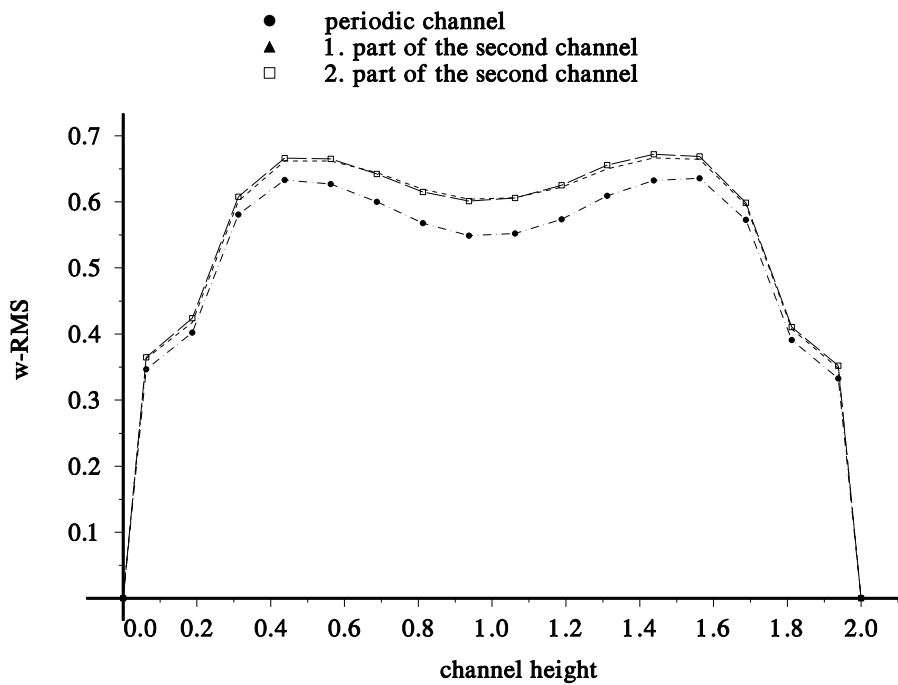


Fig. 5: w-rms, equidistant grid

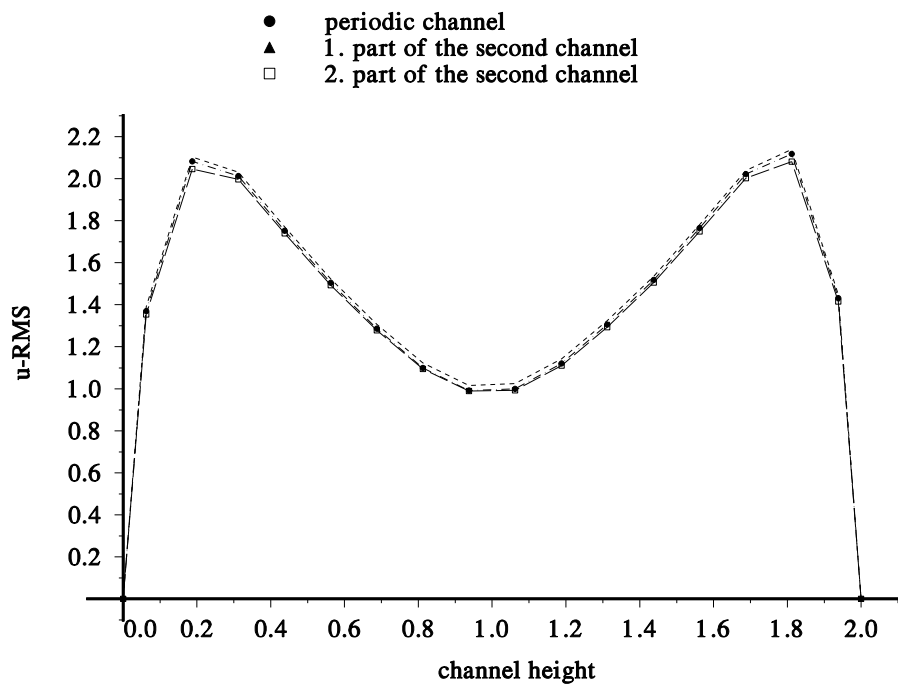


Fig. 6: u-rms, non-equidistant grid

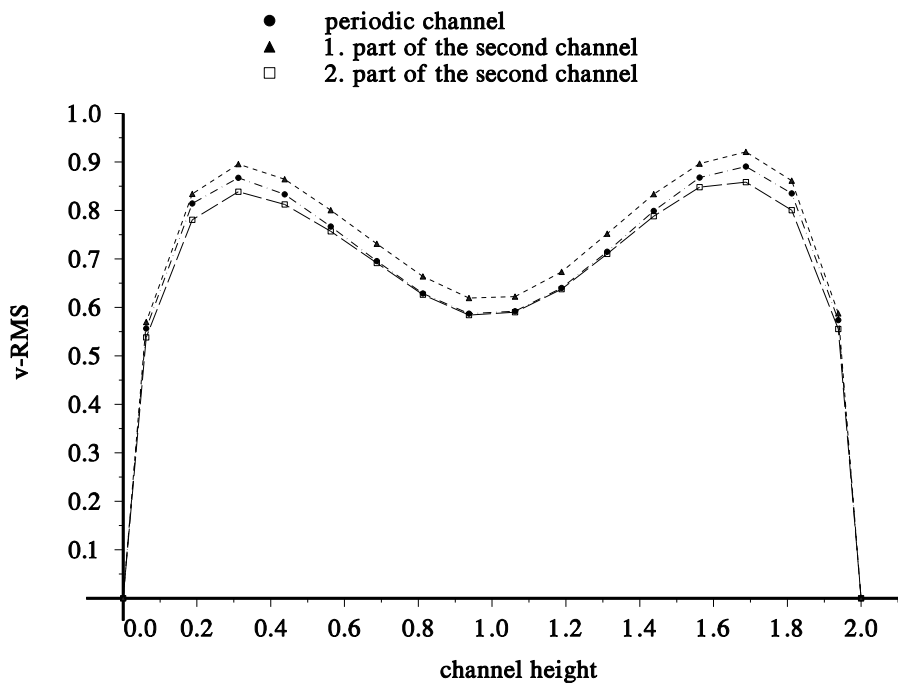


Fig.7: v-rms, non-equidistant grid

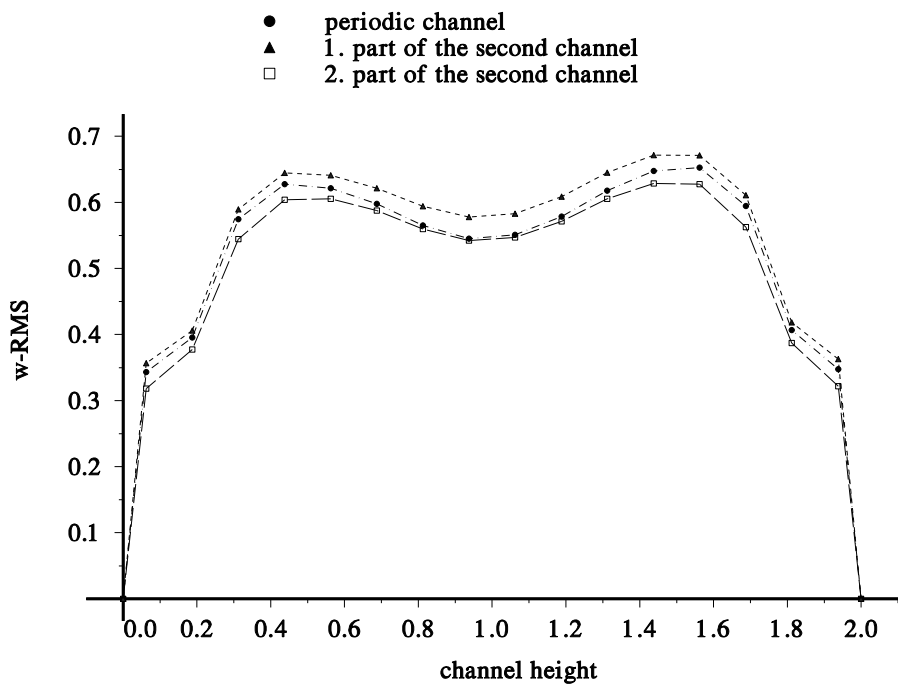


Fig. 8: w-rms, non-equidistant grid

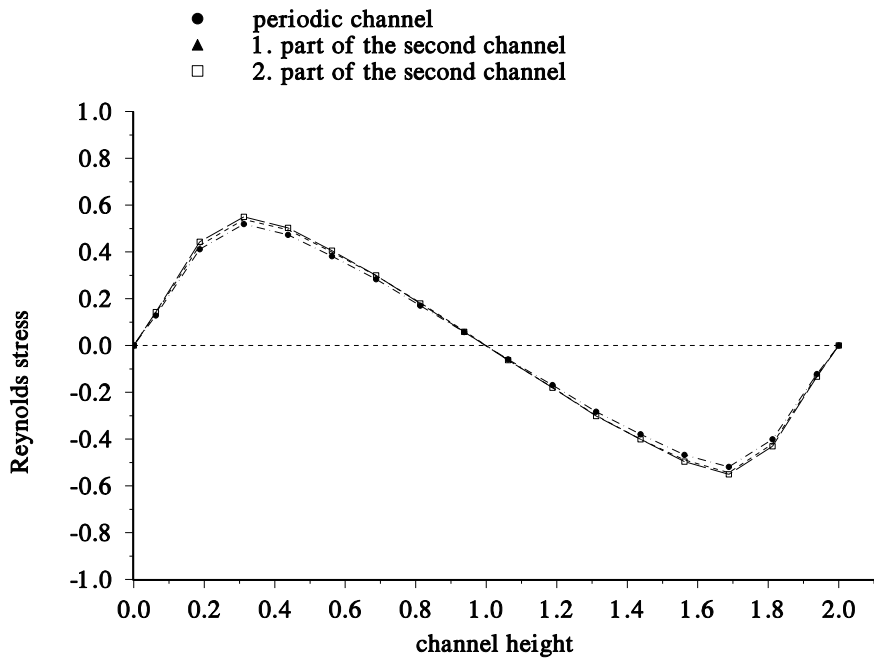


Fig. 9: Reynolds stresses (uw-component in  $xz$ -plane)

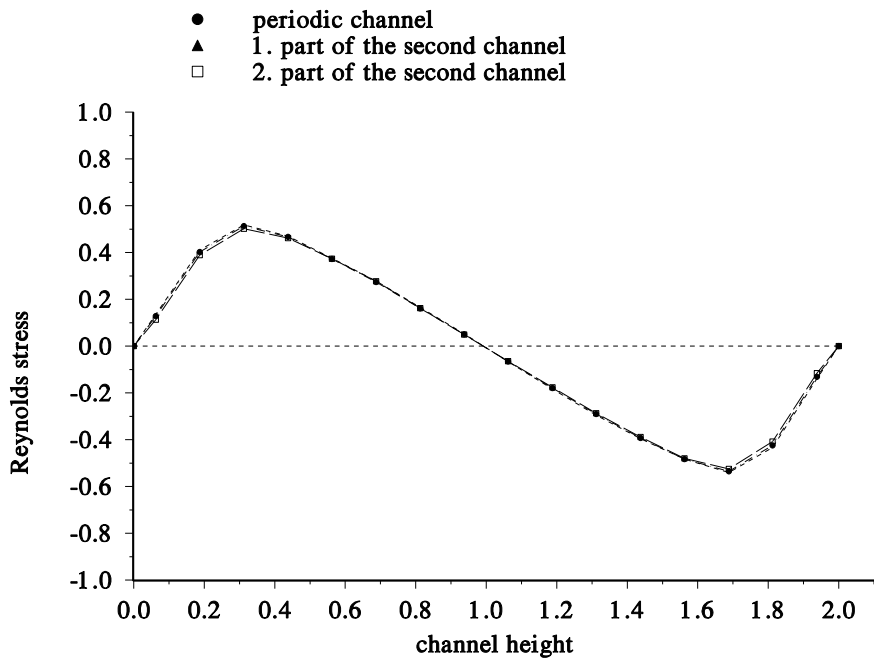


Fig. 10: Reynolds stresses (uw-component in  $xz$ -plane)

		periodic channel	1. part testchannel	2. part testchannel	difference of 1. part	difference of 2. part
u-rms	min	1.028	1.075	1.067	4.85%	3.88%
	max	2.112	2.146	2.154	1.61%	1.99%
v-rms	min	0.584	0.644	0.643	10.27%	10.10%
	max	0.883	0.924	0.928	4.64%	5.10%
w-rms	min	0.549	0.604	0.601	10.02%	9.47%
	max	0.635	0.666	0.672	4.88%	5.83%
Reynoldsstress	min	-0.519	-0.543	-0.551	-4.62%	-6.17%
	max	0.529	0.554	0.550	4.73%	3.97%

**Table 1:** Comparison of local maxima (max) and minima (min) for different 1D-ensemble-averaged values, **equidistant grid** (averaging was done in  $x$ - and  $y$ -direction; the differences of each part of the second (test-) channel expressed in percent are referred to the values of the periodic channel)

		periodic channel	1. part testchannel	2. part testchannel	difference of 1. part	difference of 2. part
u-rms	min	0.992	1.016	0.989	2.42%	-0.30%
	max	2.117	2.139	2.081	1.04%	-1.70%
v-rms	min	0.587	0.620	0.584	5.62%	-0.51%
	max	0.891	0.921	0.859	3.37%	-3.59%
w-rms	min	0.545	0.578	0.542	6.06%	-0.55%
	max	0.653	0.671	0.629	2.76%	-3.68%
Reynoldsstress	min	-0.535	-0.540	-0.526	-0.93%	1.68%
	max	0.513	0.518	0.501	0.97%	-2.40%

**Table 2:** Comparison of local maxima (max) and minima (min) for different 1D-ensemble-averaged values, **non-equidistant grid** (averaging was done in  $x$ - and  $y$ -direction; the differences of each part of the second (test-) channel expressed in percent are referred to the values of the periodic channel)

	periodic channel	1. part testchannel	2. part testchannel	difference of 1. part	difference of 2. part
Centerline-velocity	18.65	18.57	18.54	-0.43%	-0.59%

**Table 3:** Comparison of the averaged Centerline-velocities, **equidistant grid**

	periodic channel	1. part testchannel	2. part testchannel	difference of 1. part	difference of 2. part
Centerline-velocity	18.58	18.51	18.48	-0.53%	-0.53%

**Table 4:** Comparison of the averaged Centerline-velocities, **non-equidistant grid**